Hot Deformation Behaviors of Low Carbon Steels

Chainarong Srikunwong*

*Department of Mechanical Engineering, Faculty of Engineering, King Mongkut's Institute of Technology North Bangkok, Bangsue, Bangkok 10800, Thailand,
Tel.: +66 (0) 90755752, Fax: +66 (0) 25869541, E-mail: csw@kmitnb.ac.th,

Abstract

The present paper outlines an understanding of some fundamentals of flow behavior substantial practical tests and issues. A number of hot compression tests was performed at various isothermal conditions and strain rates in order to simulate the flow behavior of low carbon steel grades. Thermomechanical simulator, namely Gleeble®-3500, was utilized conducting the tests.

Results were discussed in terms of the influence of temperature and that of strain rate on flow behavior of low carbon steels. A power-law viscoplastic model was proposed to characterize the flow behavior and a comparison between experimental results and that predicted was made.

Keywords: Hot compression test, Low carbon steels, Viscoplastic model

1. Introduction

In recent years, advanced metal forming process has emerged as one of the most important fabrication techniques in terms of competitiveness and cost of the process compared with machining, sintering, or casting process. Sheet forming associated with the plastic flow of metals has been transformed from the conventional fabrication to the advanced 'state of the art' process.

However, many aspects involved different process mechanisms must be taken into account as far as possible, such as strain hardening, viscoplastic flow, evolution and final microstructures, the damage, the heat transfer between workpiece and tool, the elastic deformation of dies, and also the friction or lubrication conditions at tool/metal interface. Basing on these production aspects, low carbon steels present the outstanding mechanical characteristics and have being commonly used as the established material for autobody fabrication due to their privileged formability potential.

Concerning weldability in resistance spot welding-(RSW), dominant joining technique used in body-in-white-(BIW) fabrication, such steels present an exceptional weldability with good mechanical performance, and fatigue strength of the welds.

Owing to the widely use of these steels in automotive industry, several studies of process modeling have been devoted to both multi-stage forming [1], and welding process [2]. Especially for welding simulation, the mechanical behaviors of steels as a function of temperature ranging from room temperature to fusion are fundamental databases of material properties in a finite element code. Because of the lack of stress/strain relationship of steels at elevated temperature in our mechanical database for welding simulation, the aim of this research is to study and model the hot deformation behavior of low carbon steels.

A general experiment guideline can be highlighted in order to specify the test conditions at elevated temperature such as the temperature ranges of the application, the minimum/maximum deformations, and the strain rates occurring in the workpiece. There are three experimental techniques for elevated temperature material behavior study, which are the hot tensile, compression [3], and torsion test [4]. However, hot tensile test seems suitable for small deformation process modeling. Since it suffers from a limitation, which is the appearance of the instability before reaching higher strain region. In the case of low carbon steels, the conventional elongation can attain typically 20-30% before striction. Hot compression and torsion tests become better choices to study the flow behavior for large deformation process. Strain resulting from both tests can attain 0.5-1.0. In this study, a thermomechanical simulator, namely Gleeble®-3500 of DSI, is employed for steel behavior simulation. However for such a test, an universal tensile/compression testing machine equipped a furnace provides also a possibility to perform the upset compression test at elevated temperature.

Chemical compositions of low carbon steels, namely Al-Killed Drawing Quality-(AKDQ), and Interstitial Free-(IF) steel grades are given in Table 1. Light optical microscopy observation in Figures 1a-b displays typical microstructures in the base metal of AKDQ and that of IF steel prior to experiment.

Table 1. Chemical compositions of IF and AKDQ steels: (10^{-3}% wt)

Materials	*C*	*Mn*	*P*	*S*	*Si*	*Al*	*Ni*	*Cr*	*Cu*	*Nb*	*V*	*Ti*	*B*	*Mo*	$C_{eq\text{-}IIW}$ [5]
1. IF	1.9	102.6	11.7	8.5	13.6	38.4	14.5	19	13.4	0.2	1.8	78	0.021	0.8	27.4
2. AKDQ	28.8	202.2	9	11.8	6.9	41.1	15.2	18	16.7	0.3	0.5	0.5	0.018	0.7	69.6

Note: $C_{eq-IIW} = C + \frac{Mn+Si}{6} + \frac{Cr+Mo+V}{5} + \frac{Ni+Cu}{15}$

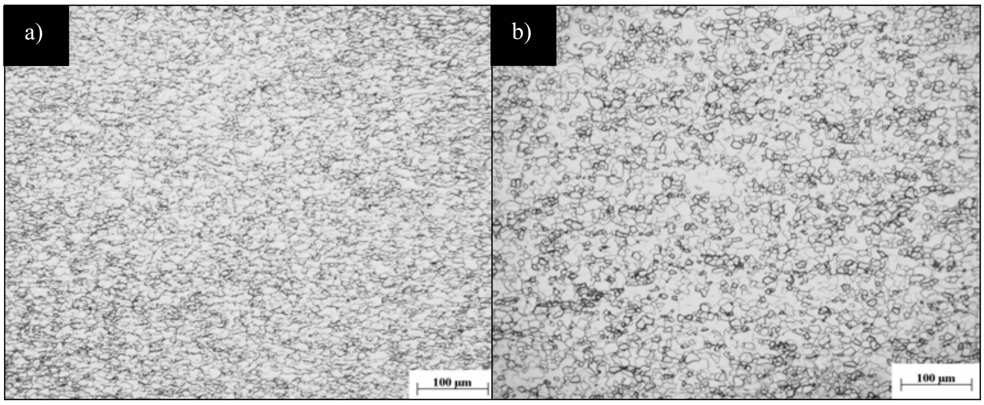

Figure 1 Light optical microscopy observation of steels utilized in this study-(Nital etch-5%), a) Microstructures of the base metal of AKDQ steel, and b) Microstructures of the base metal of IF steel

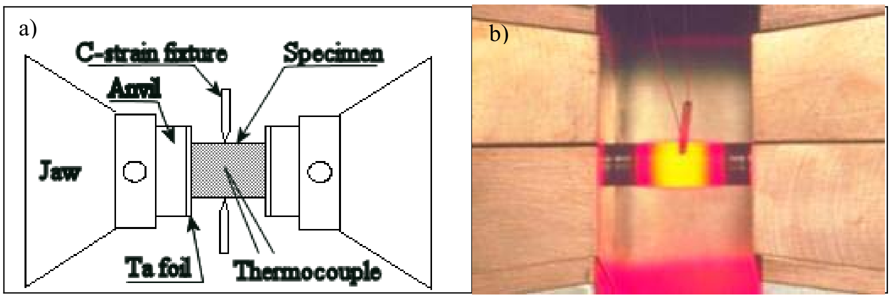

Figure 2 Axial hot compression test, a) Schematic illustration of a specimen and measurement devices in Gleeble® machine, and b) An isothermal compression test carried out at 1200°C.

2. Experimental Procedures

Heating rate of 5°C/s and specimen dimension are based on the recommendation of DSI documented in the application notes [6]. This is to assure an isothermal condition in the entire specimen.

Cylindrical specimens of 10-mm diameter and 12-mm height are prepared. Tantalum foils being used as lubricant are inserted at the anvil/specimen interfaces as shown in Figure 2a. Tantalum foil can prevent not only interface sticking, but also helps reducing the specimen *bulging* produced by the interfacial friction and thus ensure a homogenous deformation of the cylindrical specimen. It is noted that one of the compression test principles is to maintain an instantaneous uniform sectional area of specimen during the test, without the occurrence of bulging or barreling of the cylindrical specimen. Friction or barreling effect can be considered as one of the critical issues for compression test. To avoid this phenomenon, an excellent lubrication at the interface is indispensable. A test performed at 1200°C is shown in Figure 2b. In fact, we desired to perform the test at the highest temperature as possible, e.g. at 1500°C, but when temperature is greater than 1200°C, the specimen commences softening and its cylindrical shape is not completely conserved.

Experiments are carried out at four different strain rates of 0.01, 0.1, 0.2, and 0.5 s^{-1}, respectively. C-strain gauge mounted at mid-specimen length allows measuring the change in diameter of cylindrical specimen, or output deformation. Imposed strain and heating rates are piloted by the user's program and they are supervised by computer-controlled system of Gleeble® machine. A microthermocouple is welded at the half of specimen length for temperature measurement as shown in Figure 2b. To avoid the high temperature oxidation, all tests are performed in vacuum. For compression test, the effective strain can be calculated with the absence of the barreling:

$$\varepsilon = \ln(\frac{h_0}{h}) = 2\ln(\frac{d}{d_0}) \qquad (1)$$

where 'h' and 'h_0' are instantaneous and initial height. 'd' and 'd_0' are instantaneous and initial diameter of the specimen, respectively. In this study, we consider the diametric deformation as the measurement output to calculate an instantaneous strain.

To perform the experiment at a constant strain rate, the incremental displacement of mobile jaw of Gleeble® is programmed using the following expression for required total strain of 0.5.

$$Stroke = h_0(\exp(\dot{\varepsilon}.t) - 1) \qquad (2)$$

where '$Stroke$' is the instantaneous displacement of the mobile jaw, '$\dot{\varepsilon}$' is the prescribed strain rate, and 't' is time.

3. Model Description

Generally, the criteria for the mechanical behavior model selection are based on process characteristics, which are temperatures in service, strain rates, total and isotropic/anisotropic deformations of those materials found in the process. However, other criteria concerned practical aspects like the number and type of experiments needed to establish a model. These issues become a decisive condition concerning time/cost effectiveness for the experiments to evaluate model parameters. In the case of numerous parameters presenting in the model formulation, a numerical method is sometimes useful to optimize a set of appropriate parameters in order to correlate model and experimental results. In this study, an isotropic power-law viscoplastic model is selected and can be stated for the inelastic strain rate as follows [7]:

$$\underline{\underline{\dot{\varepsilon}}}^p = \frac{\partial \Omega}{\partial \underline{\underline{\sigma}}} = \frac{3}{2}\dot{\varepsilon}^p_{eq}\frac{\underline{\underline{s}}}{\sigma_{eq}} \qquad (3)$$

where the deviator of Cauchy stress tensor is $\underline{\underline{s}} = \underline{\underline{\sigma}} - \frac{1}{3}Tr(\underline{\underline{\sigma}})\underline{\underline{I}}$. '$\Omega$' is the viscoplastic potential. Equivalent plastic strain rate is:

$$\dot{\varepsilon}^p_{eq} = \left(\frac{2}{3}\underline{\underline{\dot{\varepsilon}}}^p : \underline{\underline{\dot{\varepsilon}}}^p\right)^{1/2} = \left(\frac{\sigma_{eq}}{k.\varepsilon^{p\,n}_{eq}}\right)^{1/m} \qquad (4)$$

Power-law viscoplastic model becomes:

$$\sigma_{vp} = k.\varepsilon^{p\,n}_{eq}.\dot{\varepsilon}^{p\,m}_{eq} \qquad (5)$$

Finally, introducing von-Mises criterion for metallic material behavior with the unidirectional formulation, stress/strain relationship is:

$$\sigma_{VM} = \sigma_s + k.\varepsilon^n.\dot{\varepsilon}^m \qquad (6)$$

where 'σ_s' is the initial elastic limit stress. 'k' and 'm' are the material constant and strain rate sensibility, respectively. 'n' is the work hardening coefficient. These coefficients are described as a temperature dependent function. It is evident according to the formulation that three tests along with different strain rates at an isothermal condition have to be performed in order to determine model parameters.

Other empiric formulation for creep behavior at high temperature can be found in the pioneer work of Sellars-Tegart [8], (e.g. when $T > 1/3.T_f$, the creep behavior in metals can be observed). This sinh-Arrhenius constitutive model is developed based on the energy balance principle between work hardening and softening originated from the dislocation multiplication and annihilation during hot deformation:

$$\dot{\varepsilon} = A(\sinh \alpha\sigma)^q \exp(-Q/RT) \qquad (7)$$

Where 'Q' and 'T' are the activated energy of deformation and absolute temperature, respectively. 'R' is the universal gas constant. 'A' and 'α' are constants. 'q' is the strain rate sensitivity parameter. This model is suitable for modeling a high temperature flow behavior.

The independence of stress function decoupled between strain and strain rate in (5) allows determining the model parameters.

Work hardening coefficient:

$$n = \left.\frac{\partial \ln \sigma_{vp}}{\partial \ln \varepsilon}\right|_{\dot{\varepsilon},T} \qquad (8.1)$$

Strain rate sensibility coefficient:

$$m = \left.\frac{\partial \ln \sigma_{vp}}{\partial \ln \dot{\varepsilon}}\right|_{\varepsilon,T} \qquad (8.2)$$

Note that $0 < m \leq 1$. Total strain associating with elastic and viscoplastic strains ('ε_e' and 'ε_{vp}', respectively) can be given as follows:

$$\varepsilon_{tot} = \varepsilon_e + \varepsilon_{vp} \qquad (9)$$

For hot compression test with moderate or high strain rates as in our case, it is not easy to determine the elastic strain from the experimental curves. However, the relationship of Young's modulus, model parameters, and elastic strain can be established as follows:

$$\varepsilon_e = \left(\frac{k.\dot{\varepsilon}^m}{E}\right)^{\frac{1}{1-n}} \qquad (10)$$

Equation (10) is derived similarly to those proposed by Morrison [9] for the determination of elastic strain of Hollomon elastoplastic model. Young's modulus of low carbon steels as a function of temperature is given in the metals handbook [10]. It is proved analytically that the elastic deformation or yield stress depends only on strain rate at an isothermal condition. Furthermore, it is well known according to the experience that the higher the strain rate, the greater the yield stress. Strain rate has no influence on Young's modulus at a given temperature.

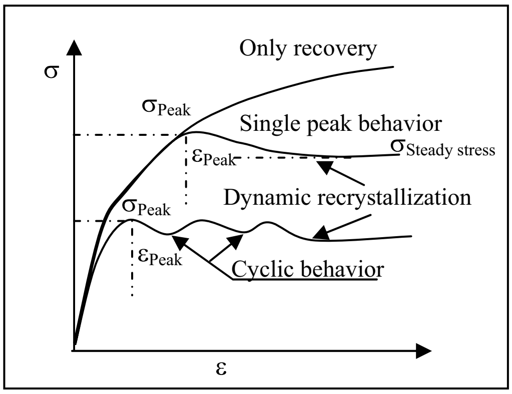

Figure 3 Schematic representation of flow behavior at elevated temperature [11]

4. Results and Discussion

Flow Stress Behaviors at Elevated Temperature:

An introduction of three successive stages of hardening/softening mechanisms observed on flow stress curves of austenitic steels at elevated temperature is illustrated in Figure 3. The first stage is concerned the combined *hardening* and *recovery* mechanisms at small deformation. This stage is characterized by the multiplication of dislocation density, the elongation of primary grains, and the development of the secondary or sub-grains in the primary deformed grains. During this stage, however, there are no new grains created. From a microstructural point of view, there is only a reduction of atomic defaults with a new arrangement of stacking faults, especially that of dislocations.

Two latter stages are separated by a transition zone appearing between peak and steady state stress. Softening mechanism due to *dynamic recrystallization* can be observed in two different ways: single peak flow stress observed at low temperature and high strain rates, and multiple-peak stress at high temperatures and/or low strain rates. For carbon steels, other factors that can influence directly on flow behaviors are carbon, and silicon content.

In this study, the dynamic recrystallization with multiple peak stresses can be markedly observed on the flow curves of both IF and AKDQ steels at 1100, and 1200°C, particularly at low strain rate of 0.01 s^{-1}, as illustrated in Figures 4a-b.

At elevated temperature with higher strain rates, e.g. 0.2 and 0.5 s^{-1} in Figure 4, stress flow curves of both steels show single peak behavior. However, critical deformation, 'ε_p', of IF steel is found to be more significant than that of AKDQ steel.

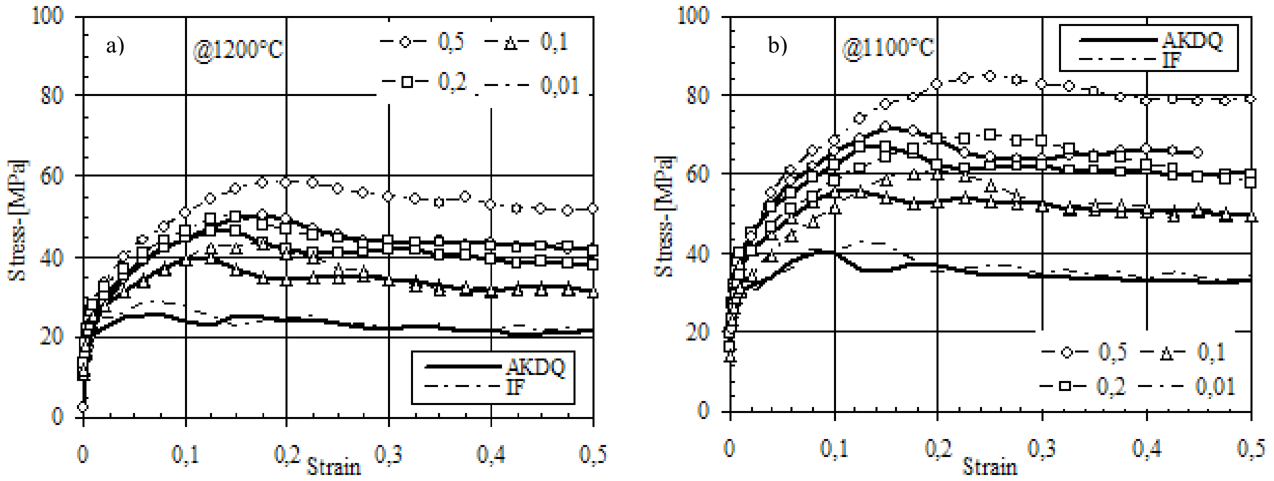

Figure 4 Influence of temperature and strain rate on flow stress of AKDQ and IF steels at elevated temperature, a) Flow stress vs. strain rate at 1200°C, and b) Flow stress vs. strain rate at 1100°C

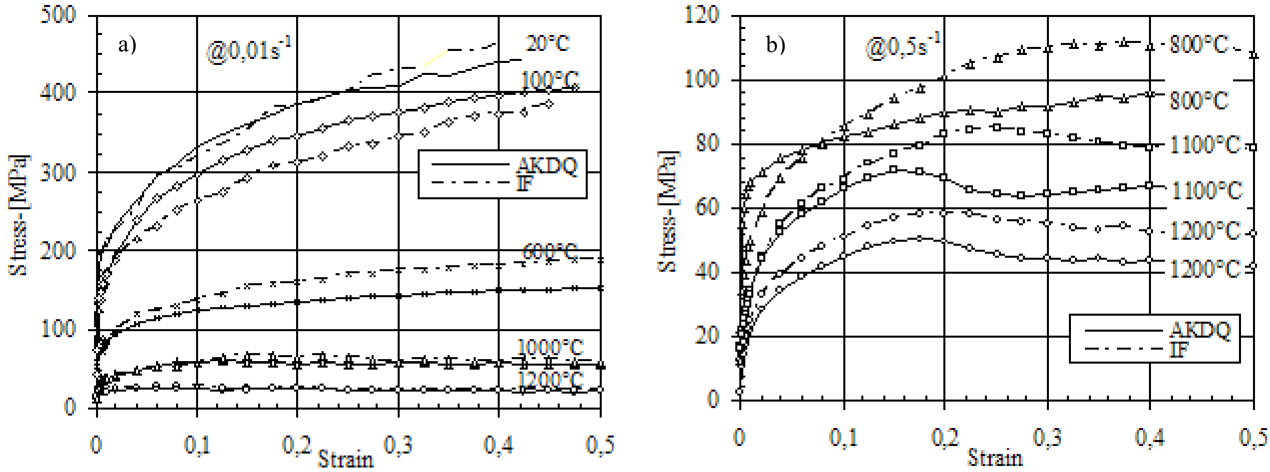

Figure 5 Illustration of stress/strain vs. temperature comparing between IF and AKDQ steel grades, a) Influence of temperature on flow stress@ 0.01 s^{-1}, and b) Influence of temperature on flow stress at elevated temperature@0.5s^{-1}

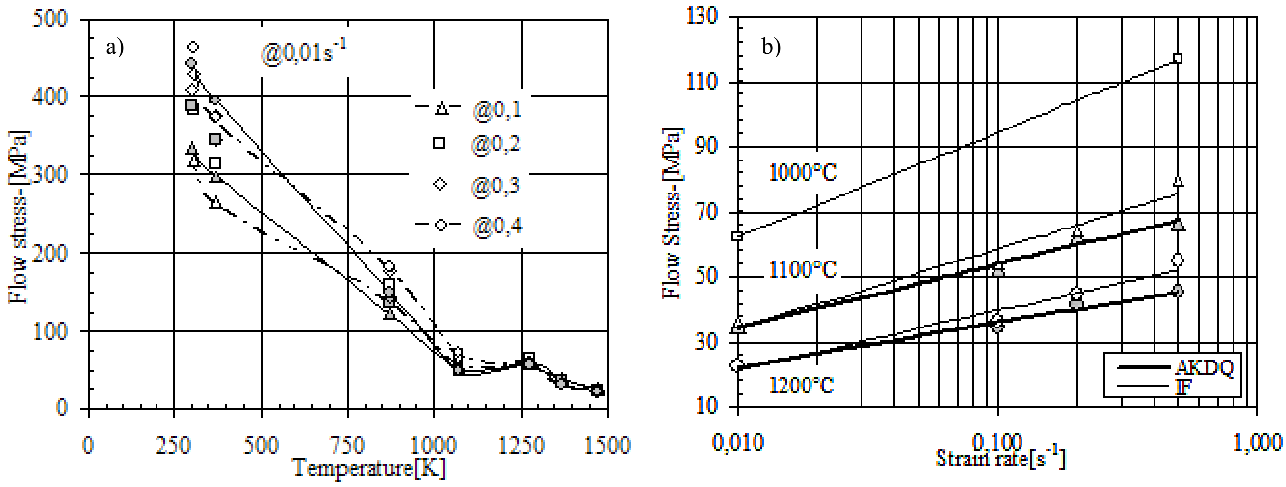

Figure 6 Illustration of flow stress characteristics, a) Flow stress of steels considered at ε= 0.1, 0.2, 0.3, and 0.4 @ 0.01s^{-1}-[Grey and white symbols are represented for AKDQ, and IF steel case, respectively], and b) Influence of strain rate on steady state flow stress, 'σ_{ss}'

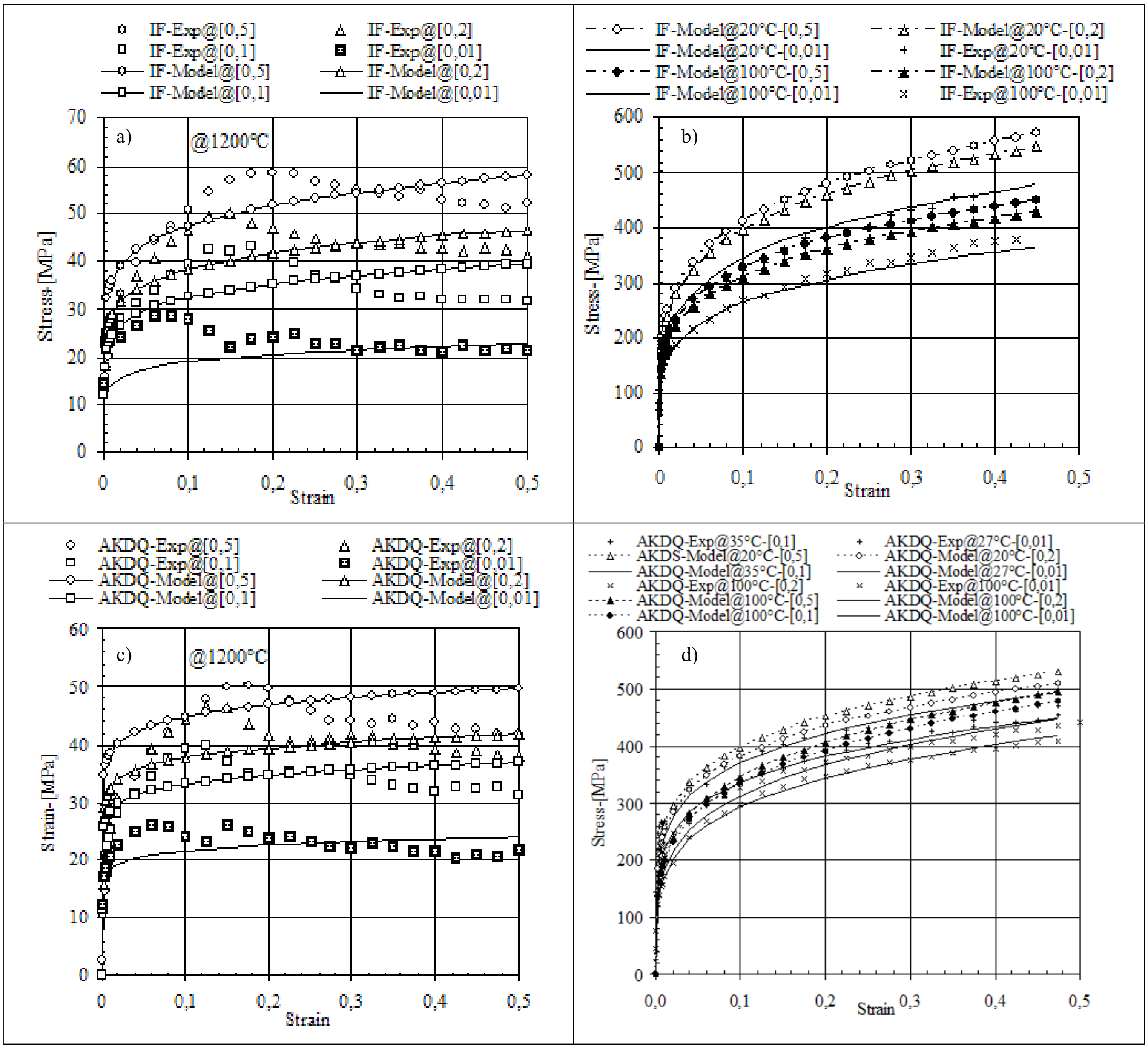

Figure 7 Stress-strain relationship as a function of strain rate predicted by the model and that obtained from experiments-[strain rate is indicated in the bracket], a) IF steel@1200°C, b) IF steel@20 and 100°C, c) AKDQ steel@1200°C, and d) AKDQ steel@20°C and 100°C-[A consequence of compression with high strain rate is the increase of temperature in the specimen. Therefore, average temperature is indicated in Figure 7d]

Temperature Effect on Flow Stress:

Typical flow stress curves presented in Figure 5a show the influence of temperature on flow stress at retained strain rate of 0.01 s^{-1}. It is disclosed that stress decreases drastically when temperature increases as displayed in Figure 6a. At elevated temperature, plastic flow behavior of both steels can be observed. Influence of temperature on flow stress for 0.5 s^{-1} illustrated in Fig. 5b indicates that flow stress of IF steel is slightly higher than that of AKDQ steel at elevated temperature.

Strain-Rate Effect on Flow Stress:

Comparing stress-strain curves between the same steel grade depicted in Figures 7a and b, it is revealed that the increase in strain rate results, evidently, the increase in flow stress. As mentioned in the previous section, strain rate has the influence not only on flow stress, but also on yield stress as demonstrated in (10).Influence of strain rate on steady state stress at elevated temperature can be found in Figure 6b. It can be suggested from experimental results that increases in strain rate will result in higher steady state stresses.

Prediction of Stress-Strain Curves:

Comparison between stress-strain curves obtained from the experiments and that of prediction can be found in Figure 7. For all applied strain rates, it is evident that the proposed viscoplastic model can predict accurately flow stress behavior at low and intermediate temperatures as shown in Figures 7b and 7d.

Accordingly, the nature of power-law model cannot well simulate the softening mechanisms at elevated temperature with moderate and high deformation rates. However, steady stress with relative low strain rate can be effectively characterized with the use of this model as in the case of 1200°C@0.01 s^{-1} depicted in Figures 7a, and 7c. Figure 8a shows a prediction of stress-strain curves as a function of temperature at strain rates of 0.01 and $0.5s^{-1}$.

Engineering yield stresses, Young's modulus as a function of temperature incorporating the influence of strain rates can be seen in Figure 8b. Yield stress of low carbon steel decreases linearly with temperature. It is observed that yield stress of AKDQ steel is slightly higher than that of IF steel.

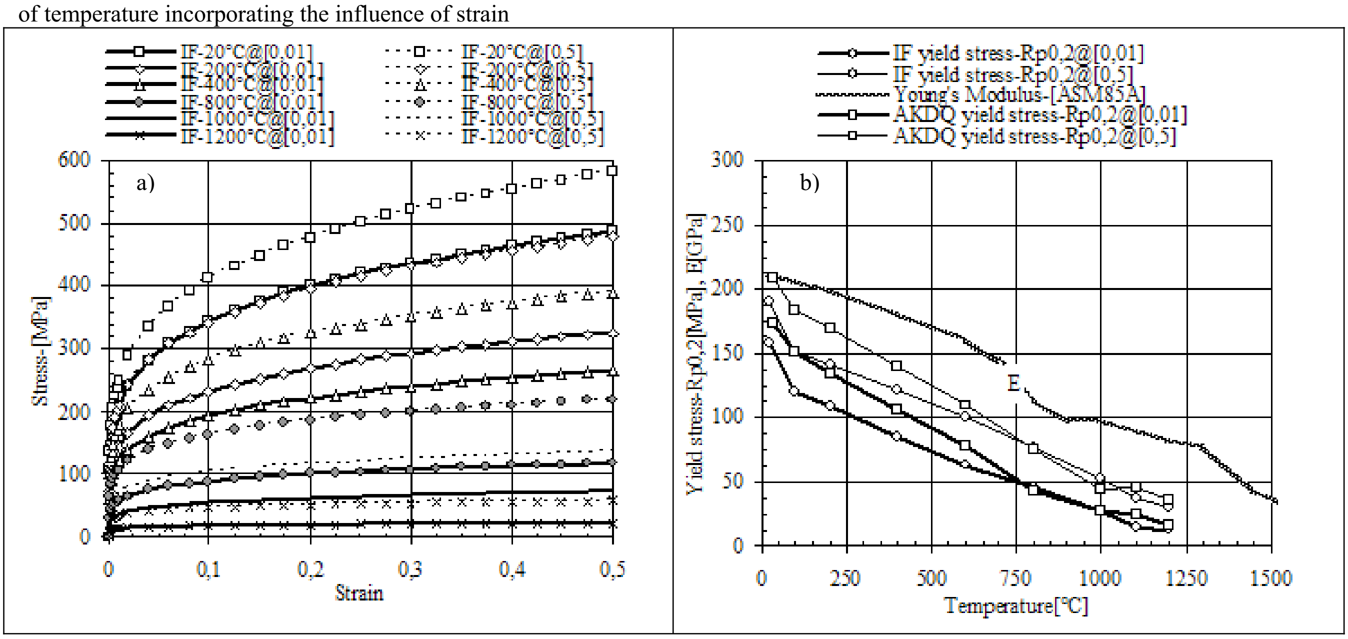

Figure 8 Prediction of stress-strain relationship and engineering yield stress, $R_{P0,2}$, as a function of temperature with the use of viscoplastic model, a) Stress-strain curves predicted@ 0.01 to $0.5s^{-1}$, and b) Prediction of engineering yield stress as a function of temperature for both steels

5. Concluding Remarks

Hot deformation behaviors of low carbon steels are studied employing hot compression simulation technique. A viscoplastic model is used characterizing these experimental data. Following conclusions can be drawn from this research:

i) Temperature has a dominant role on stress; stress decreases when temperature increases. Increasing strain rate promotes higher both yield and flow stresses. Hardening and softening mechanisms can be observed on flow behavior curves of low carbon steels at elevated temperature.

ii) Power-law viscoplastic model yields comparable results with the flow behavior experimental data at room and intermediate temperatures. Established model and experimental data of these steels obtained from this study are useful for ongoing numerical simulation of welding process. This model takes into account the influence of temperature as well as that of strain rate on the mechanical behavior.

To model efficiently the flow behavior of steels at elevated temperature, the existing sinh-Arrhenius model can well characterize the deformation history effects associating with softening mechanisms in steels. However, power-law viscoplastic model enables to predict the steady state flow stress with low strain rate at elevated temperature.

Acknowledgement

The author would like to thank Dr. Dominique CORNETTE, the head of client cluster service of IRSID, Groupe Arcelor-France, for his input and support. Mr. Eric COLLIER of Sollac Atlantique de Dunkerque-France, is acknowledged for technical assistance. Partial financial fund of Association Nationale pour la Recherche et la Technologie (CIFRE educational program) through contract with Centre des Matériaux P-M Fourt, Ecole des Mines de Paris is gratefully acknowledged.

References

[1] Sala, G., 2001, A Numerical and Experimental Approach to Optimise Sheet Stamping Technologies, Materials and Design, 22, pp. 285-298.

[2] Srikunwong C., Dupuy T., and Bienvenu Y., 2003, Influence of Electrical-Thermal Physical Properties in Resistance Spot Welding Modelling, Mathematic Modelling of Weld Phenomena VII, Cerjak H. *et al.* eds., The Institute of Materials London.

[3] Jonas, J.J., Sellars, C.M., and McG. Tegart, W.J., 1969, Strength and Structure under Hot Working Conditions, Metallurgical Reviews, 130, pp. 1-24.

[4] Rossard, C., and Blain, P., 1958, Revue Métallurgie, 55.(in French)

[5] Bailey, N., 1994, Weldability of Ferritic Steels, 1st ed., Abington publishing.

[6] Gleeble® Systems, 2000, Application Notes-APN022, Dynamic Systems Inc., NY.

[7] Lemaitre, J., and Chaboche, J.L., 1998, Mechanics of Solid Material" Cambridge University Press, 2nd ed., pp. 253-345.

[8] Sellars, C.M., and McG. Tegart, W.J., 1966, Revue Métallurgie, 63.(in French)

[9] Morrison, W.B., 1966, The Effect of the Grain Size on the Stress-Strain Relationship in Low Carbon Steel, Transaction of the ASM, 59, pp. 824-846.

[10] Physical Properties of Carbon, Low-Alloy, Stainless and Tool Steels; Metals Handbook, Metal Parks, OH., American Society of Metals, 1985, pp. 1-63.

[11] Bénard, J., Michel, A., Philibert, J., and Talbot, J., 1994, Métallurgie Générale, 2ième édition, Masson.(in French)